Digital division mask technique for improving the lithography quality of DMD-based system

ZHIMIN ZHANG[a, b], YIQING GAO[b], NINGNING LUO[a,*,b], MIN CHEN[b]
[a]*College of Automation Engineering, Nanjing University of Aeronautics and Astronautics, Nanjing 210016, China*
[b]*Key Laboratory of Nondestructive Test (Chinese Ministry of Education), Nanchang HangKong University, Nanchang 330063, China*

To decrease the high-frequency energy loss resulted from the low-pass property of reduction lens in DMD-based maskless lithography system, the digital division mask technique has been proposed. Three digital division methods have been developed to fabricate different types of microstructures, including periodic amplification division, bit coding division and the two combine. For verification of the proposed methods, simulations and experiments have been performed to fabricate binary grating, zigzag grating and other microstructures. Comparative exposure patterns reveal that these methods are versatile and reliable for improving the lithography quality of DMD-based system.

(Received March 12, 2013; accepted July 10, 2014)

Keywords: Digital division mask, Periodic amplification division, Bit coding division, Lithography quality

1. Introduction

Microstructures are of great importance for industries, such as micro-optical system, microelectromechanical systems (MEMS) and micro total analysis systems (μTAS) [1-2]. Many maskless lithography techniques have been successfully applied to the fabrication of complex microstructures. Recently, maskless lithography that utilizes digital micromirror device (DMD) as a dynamic mask has been developed to direct-write microstructures [3-5]. In comparison with other maskless lithography techniques, the DMD-based maskless lithography possesses superior features. The particular advantage of the area-write technique is that it enables the large areas of the substrate to be simultaneously direct-written, which brings about efficiency in cost and time. The second key advantage is the ability to modulate the mask pattern electronically, without physically replacing the mask, which simplifies the operation process.

For the reduction lens in DMD-based maskless lithography system [6], it can be generally regarded as a low-pass filter because of its finite transmission aperture, which consequently leads to the decline in imaging quality due to the loss of high-order diffraction. In reference [6], we reported the digital division mask technique to improve the imaging quality. Digital division mask technique is to divide an original mask obtained from the target profile into a group of binary masks. These binary masks are exposed in sequence on the same position. The target profile can be formed by the superimposed exposure of multiple binary masks. Our previous work concentrated on the feasibility vertification of digital division technique by using binary grating. However, the principle of improving image quality has not been investigated deeply. In this paper, we disclose the mechanism of improving image quality respectively for amplification division, bit coding division and the two combine. The imaging energy distribution pre and post division has been quantitatively calculated. We also consider the nonlinear intensity modulation of DMD in order to obtain the precise division masks. Simulation and experiments prove that digital division mask technique enables a more flexible and realistic profile formation with high imaging quality compared with digital grey mask technique.

2. Division methods

2.1 Method of periodic amplification division

Periodic amplification division refers to dividing an original mask into a group of binary masks by fixed or variable low-frequency period sampling. Fig. 1 illustrates the principle of periodic amplification tri-division mask. The period in each tri-division mask is three times of that in original undivided mask. If we divide original mask into N pieces of division masks, then these division masks are displayed on DMD one by one. We suppose that the intensity distribution of each division mask on photoresist is $e_i\,(i=1, \cdots, N)$, the total exposure E on the photoresist can be expressed by

$$E(x,y)=\frac{t}{N}\sum_{n=1}^{N}e_i(x,y) \qquad (1)$$

where t represents the total exposure time. Here we believe that each division mask has the same exposure time taking no account of the nonlinear effect of photoresist.

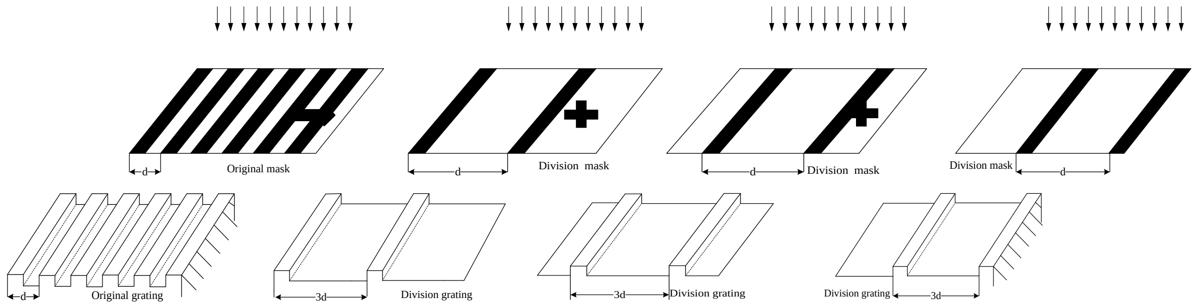

Fig. 1. Principle of periodic amplification tri-division mask.

2.2 Method of bit coding division

Bit coding division refers to dividing an original grey mask into a group of division masks by binary coding. Then division masks are exposed in sequence on the same position. The superimposed exposure of multiple binary patterns takes the place of single exposure of original grey mask. Based on the binary pulse width modulation (BPWM) of DMD, we developed bit coding division method. Fig. 2 illustrates the formation process of division masks by using a 4-bit DMD. For simplicity, only the second column on DMD is addressed.

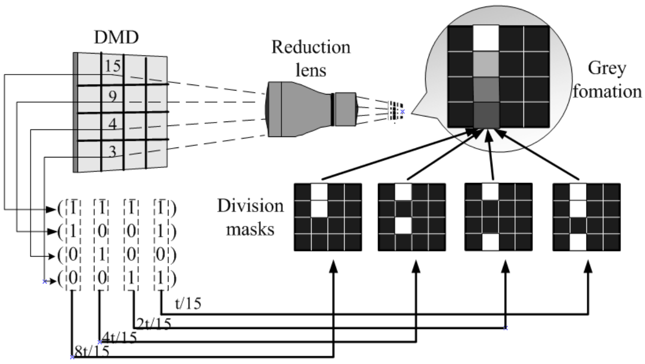

Fig. 2. 4-bit example of division masks.

Firstly, the original mask with grey values of 15, 9, 4 and 3 is transformed into 4-bit electrical words such as (1 1 1 1), (1 0 0 1), (0 1 0 0) and (0 0 1 1). And then they are input into the memory element of the corresponding micromirror, beginning with the most significant bit (MSB). Each bit in the word represents a time duration for light be on or off (1 or 0). The time durations have relative values of 2^0, 2^1, 2^2, 2^3 or 1, 2, 4, 8. The first bit (LSB) represents a duration of 1/15, the second 2/15, the third 4/15, and the MSB represents a duration of 8/15 of the video field time. Next we successively take the corresponding bits of each pixel to constitute new sequences such as (1 1 0 0), (1 0 1 0), (1 0 0 1) and (1 1 0 1), beginning with the MSB. 1 in the new sequence means that the corresponding pixel should be filled with white and 0 means the black. Each new sequence is exactly a piece of division mask. Thus Eq.(2) can be obtained by allowing for the exposure time of each division mask.

$$E(x,y)=\sum_{i=1}^{N}e_i(x,y)\cdot 2^{i-1}\cdot\frac{t}{\sum_{i=1}^{N}2^{i-1}} \qquad (2)$$

where t is the total exposure time for photoresist layer. N is the number of division masks and it's determined by the highest grey value G_{max} of the original mask, which can be calculated by Eq.(3). *Ceil* represents rounding upwards.

$$N=ceil(\log_2 G_{max}) \qquad (3)$$

2.3 Method combining periodic amplification with bit coding division

We can combine the periodic amplification division with the bit coding division as well for fabrication of some special microstructures. First, an original grey mask is divided into a group of masks (including M pieces of masks) by fixed or variable low-frequency period sampling. Then, each one in this group of masks is divided into a set of masks (including N pieces of masks) by bit coding division. Finally, we can obtain $M\times N$ pieces of division masks. These division masks are exposed in sequence on the same position.

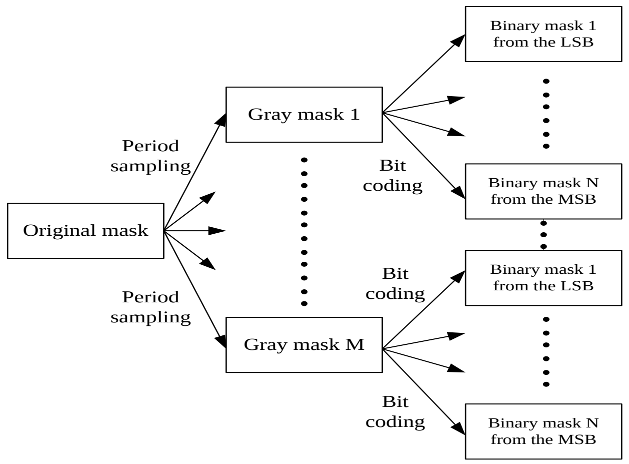

Fig. 3. Division process by combining periodic amplification with bit coding.

Fig. 3 shows the division process by combining periodic amplification with bit coding. The total exposure toward the photoresist can be given by

$$E(x,y)=\sum_{i=1}^{M}\sum_{j=1}^{N}e_{i,j}(x,y)\cdot(\frac{t}{M})\cdot 2^{j-1}\cdot\frac{1}{\sum_{j=1}^{N}2^{j-1}} \quad (4)$$

where t is the total exposure time for the photoresist layer.

3. Simulation verification

3.1. Simulation verification for periodic amplification division

The particular advantage of periodic amplification division method is that it enables more diffraction orders to pass through the reduction lens, which can improve the imaging quality effectively. The grating equation can be used to explain the idea of this method.

$$m\lambda = d\sin\theta \quad (5)$$

where m is the order number, λ is the wavelength of the light, d is the grating pitch, and θ is the diffraction angel from the DMD normal. The color variability in Fig. 4 represents the diffraction angle variation. When the grating pitch is equal to a constant (an example of d=25μm), the diffraction angle increases as the order number increases. While when the diffraction order number is equal to a constant (an example of m=50), the diffraction angle decreases as the grating pitch increases. Hence, we can conclude that the distance between diffraction orders of large-pitch mask are much closer than the distance between the orders of small-pitch mask. For a reduction lens with finite aperture, the more diffraction orders can pass through it and participate in imaging when the large-pitch mask is used. The concept of periodic amplification can therefore be seen to use multiple large-pitch masks to replace small one in lithography.

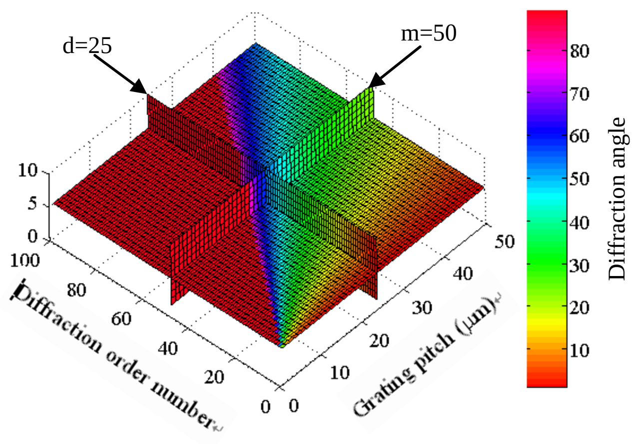

Fig. 4. Distribution of diffraction angle versus order number and grating pitch.

In order to illustrate the energy distribution variation, we calculate the results under different conditions when undivided and divided masks are respectively adopted. The original mask with grating pitch of 2μm and duty ratio of 1:2 is divided into tri-division masks with grating pitch of 6μm and duty ratio of 1:6 or 5:6. Table 1 shows the diffraction orders and diffraction energy which can be received by reduction lens.

Table 1. Diffraction orders and diffraction energy which can be received by reduction lens.

Mask	Undivided mask	Division grating mask		
		Division mask 1	Division mask 2	Division mask 3
Diffraction orders	0,±1	0,±1,±2,±3,±4,±5,±7,±8	0,±1,±2,±3,±4,±5,±7,±8	0,±1,±2,±3,±4,±5,±7,±8
Diffraction energy(duty ratio 1:6)	62.10%	62.86% (diffraction orders of 0,±1 accounting for 39.75%)	62.86% (diffraction orders of 0,±1 accounting for 39.75%)	62.86% (diffraction orders of 0,±1 accounting for 39.75%)
Diffraction energy(duty ratio 5:6)	62.10%	87.94% (diffraction orders of 0,±1 accounting for 85.35%)	87.94% (diffraction orders of 0,±1 accounting for 85.35%)	87.94% (diffraction orders of 0,±1 accounting for 85.35%)

According to Table 1, we can conclude that the diffraction orders received by the same reduction lens obviously increase from 1 to 8. For the division mask with duty ratio of 5:6, the diffraction energy involved in imaging increases from 62.10% to 87.94%. For the division mask with duty ratio of 1:6, the received diffraction energy increases inevidently. However, the energy distribution has been effectively changed. Low-frequency energy (0 and ±1) decreases from 62.10% to 39.75%, and the decreasing low-frequency energy can be considered to be transferred to high-frequency region. The diffraction energy distribution for division mask of 5:6 and 1:6 can be demonstrated by Fig.5.

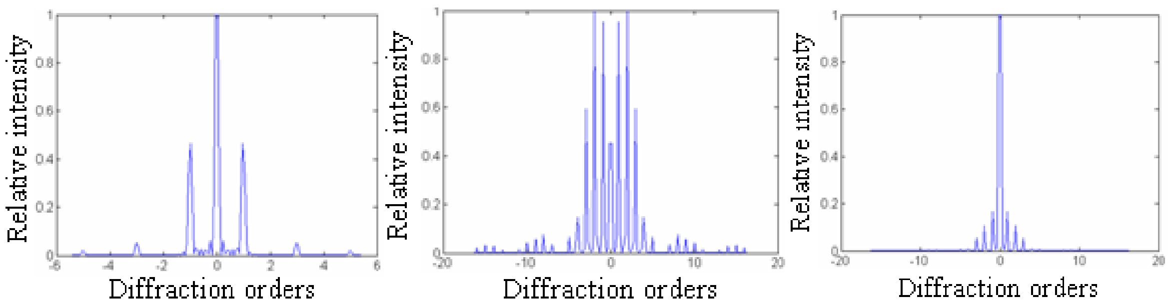

(a) Original mask (1:2) *(b) Division mask (5:6)* *(c) Division mask (1:6)*

Fig. 5. Diffraction energy distribution of original and division mask.

Fig. 6 shows the applicable grating pitch by using periodic amplification division method. In the case of tri-division grating, the diffraction intensity of original grating is gradually approaching that of tri-division grating with increasing of the grating pitch. In general, when the grating pitch is less than or equal to 8μm, the periodic amplification division method is effective. In particular, when the grating pitch is less than 3μm, the advantage of periodic amplification division method is obvious because the relative intensity difference is up to 30%.

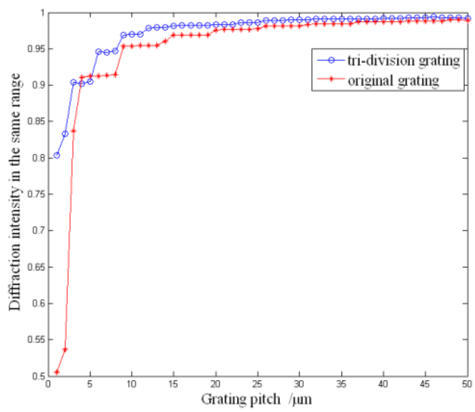

Fig. 6. Diffraction intensity comparison between original grating and tri-division grating.

3.2. Simulation verification for bit coding division

The particular advantage of bit coding division method is that it enables enhancement of high-frequency energy received by reduction lens. Commonly, the reduction lens in lithography system can be regarded as a low-pass filter because of its finite transmission aperture. Based on the diffraction-limited incoherent imaging theory, the distribution $u(x,y)$ of image field after passing by the reduction lens can be expressed by

$$u(x,y) = F^{-1}\{G(\xi,\eta)\cdot H(\xi,\eta)\} \tag{6}$$

$$G(\xi,\eta)=\sum_{m=-512}^{512}\sum_{n=-384}^{384}\left\{\left[\frac{W_xW_y}{T_xT_y}\sin c(\frac{mW_x}{T_x})\sin c(\frac{nW_y}{T_y})\cdot F(\xi,\eta)\left[\delta(\xi-\frac{m}{T_x})\delta(\xi-\frac{n}{T_y})\right]\right]\right\} \tag{7}$$

$$H(\xi,\eta)=\begin{cases}\frac{2}{\pi}\left[\arccos(\frac{\sqrt{\xi^2+\eta^2}}{2\omega_0})-\frac{\sqrt{\xi^2+\eta^2}}{2\omega_0}\sqrt{1-\frac{\xi^2+\eta^2}{4\omega_0^{\ 2}}}\right] & \xi^2+\eta^2\le 4\omega_0^{\ 2}\\ 0 & others\end{cases} \tag{8}$$

where $G(\xi,\eta)$ represents the spectrum distribution function after being sampled by DMD. $H(\xi,\eta)$ represents the optical transfer function (OTF) of reduction lens. The parameters in Eq.(6), Eq.(7) and Eq.(8) are as follows: DMD resolution is 1024×768. DMD pixel size $T_x \times T_y$ is 14μm×14μm and the effective size $W_x \times W_y$ is 13.68μm×13.68μm. $F(\xi,\eta)$ is the Fourier transformation of mask function $f(x,y)$. ω_0 is the cut-off frequency of reduction lens. If the multiple division masks are superimposed, the distribution of image field can be rewritten

$$u(x,y)=\sum_{i=1}^{N}F^{-1}\{G_i(\xi,\eta)\cdot H(\xi,\eta)\} \tag{9}$$

where *N* is the number of division masks.

Based on the above mathematical model, we calculated the energy percentage of zigzag grating in the same frequency region for original grey mask and division masks respectively. The region near the minimum frequency (zero point) in Fig.7 and Fig.8 were taken and it can be regarded as the low-frequency region. We have obtained the energy ratio of frequency components in this region to all the components. For the original grey mask, the energy ratio is 86.7% after passing by reduction lens. While for the division masks, the energy ratio is only 69.3%. So, the energy of low-frequency components decreased from 86.7% to 69.3%, which corresponds to partial low-frequency energy (17.4%) being transferred into high-frequency parts. The above data shows that bit coding division method can enhance the high-frequency energy carrying edge information. Consequently, this method can be used to improve the edge sharpness and enhance the imaging quality.

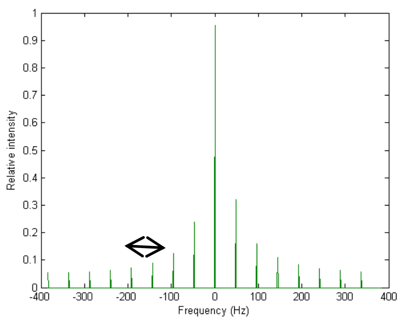

Fig. 7. Energy distribution of original mask.

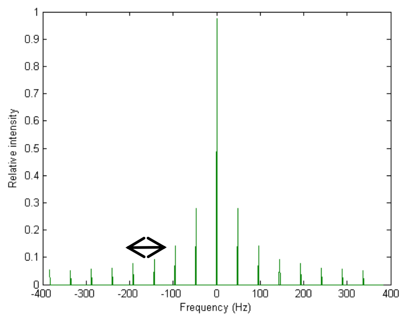

Fig. 8. Energy distribution of division masks.

The third method combines periodic amplification with bit coding division, so it has advantages of the former two methods.

4. Experimental verification

4.1 Periodic amplification division for microstructure fabrication

Binary grating with pitch of 4μm has been fabricated to verify the periodic amplification division method. Two aspects should be considered when choosing the number of division masks: one is the division effect and the other is the fabrication efficiency. Otherwise, the division effect is not obvious or the fabrication efficiency is decreased. The tri-division masks with duty ratio 5:6 and 1:6 have been designed as shown in Fig.9. The pitch of tri-division grating mask is two times than that of the original grating mask. For the undivided mask, the reduction lens can only receive five orders by calculation. While for the division mask, the reduction lens can receive sixteen orders. In exposure process, for the division masks with duty ratio of

5:6, the total exposure time is 18s and the exposure time of each division mask is 6s. For the division masks with duty ratio of 1:6, the total exposure time is 24s and the exposure time of each division mask is 8s. Fig.10 shows the lithography patterns by using undivided mask and division masks respectively. In comparison with lithography pattern by using the undivided mask, the edge of grating in Fig. 10(b), Fig. 10(c), Fig. 10(e) and Fig. 10(f) are much distinct and the line uniformity is much better by using the superimposed exposure of multiple division masks.

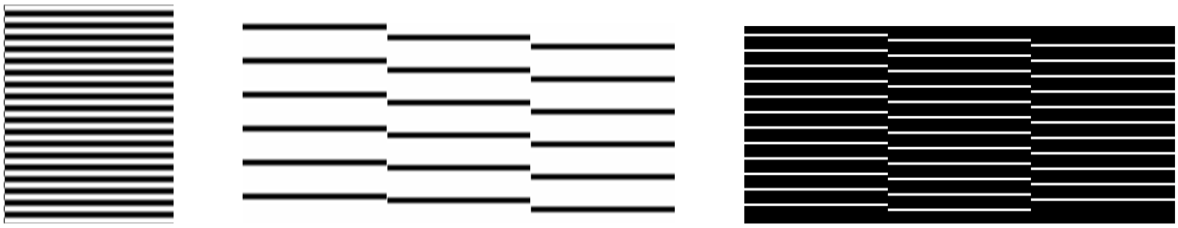

(a) Undivided mask *(b) division masks (duty ratio 5:6)* *(c) division masks (duty ratio 1:6)*

Fig. 9. Undivided mask and periodic amplification division masks.

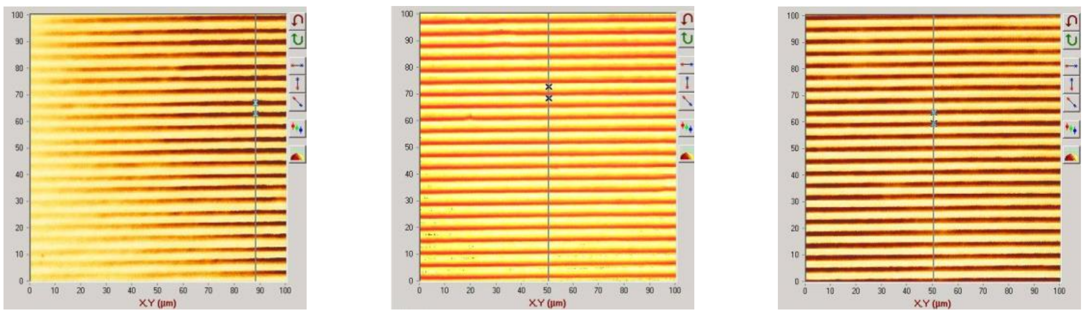

(a) Lithography pattern by using undivided mask *(b) Lithography pattern by using division masks (5:6)* *(c) Lithography pattern by using division masks (1:6)*

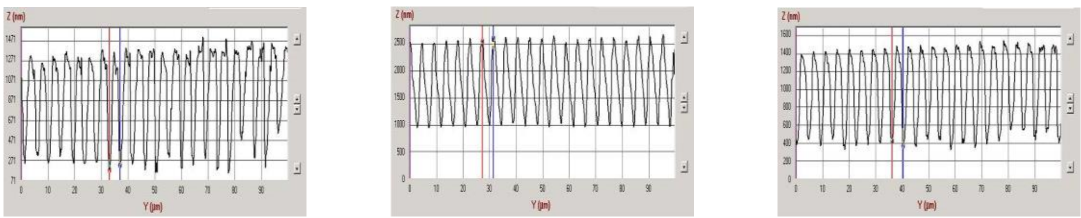

(d) 2D grating profile by using undivided mask *(e) 2D grating profile by using division masks (5:6)* *(f) 2D grating profile by using division masks (1:6)*

Fig. 10. Lithography patterns by using undivided and division masks.

4.2 Bit coding division for microstructure fabrication

To achieve the precisely controlled superimposed exposure, the original 2D grey mask should be calculated rigorously on the basis of the DMD modulation characteristic. With regards to this, we obtained the DMD modulation curve by taking the grey step 5 ranging from 0 to 255, as shown in Fig. 11. The testing curve shows the light modulation of DMD is nonlinear from 0 to 255, which causes the nonlinear change of height when the linear change of grey values is chosen. It is worth noting that the nonlinear choice of grey values will yield the irregularity of division masks. Fig. 10 shows the bit coding division masks of zigzag grating with 16μm pitch, choosing the linear region in Fig. 11. Fig. 12(a) is from the

LSB, Fig. 12(b) from the second bit, Fig. 12(c) from the third bit and Fig. 12(d) is from the MSB. According to Eq.(2), the exposure time of each division masks is 3s, 6s, 12s and 24s, corresponding to Fig. 12(a)~(d). Fig.13 shows the bit coding division masks of 3×4 truncated cone array with 100μm diameter, which is strictly calculated according to Fig. 11. Fig. 13(a)~(h) are the division masks from each bit, beginning with the LSB. In exposure process, the total exposure time is 51s and the exposure time of each division masks is 0.2s、0.4s、0.8s、1.6s、3.2s、6.4s、12.8s 和 25.6s, corresponding to Fig. 13(a)~(h). All the division masks can be exposed in sequence from MSB mask to LSB mask or from LSB to MSB. The lithography results of zigzag grating are shown in Fig. 14. Fig. 15 shows the lithography patterns of one time exposure and division exposure respectively. All the lithography photographs by division exposure reveal that the uniform patterns with distinct edge are achieved.

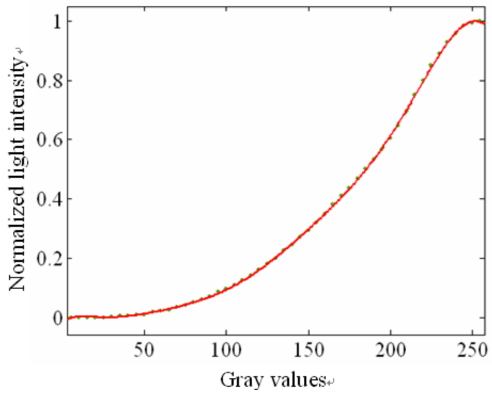

Fig. 11. DMD modulation curve.

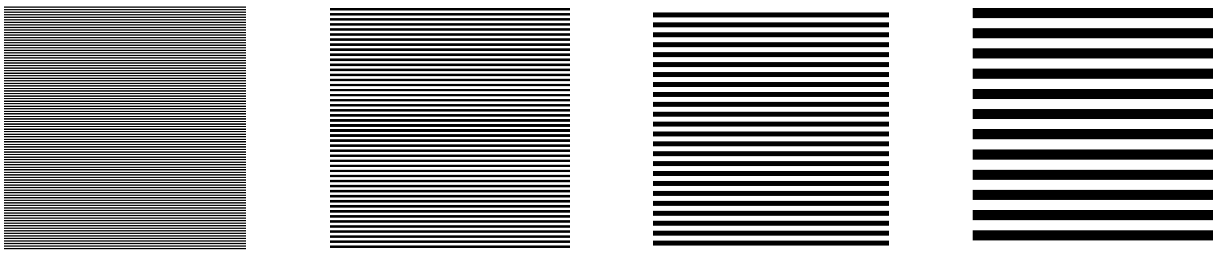

(a) division mask 1 *(b) division mask 2* *(c) division mask 3* *(d) division mask 4*

Fig. 12. Division masks for zigzag grating.

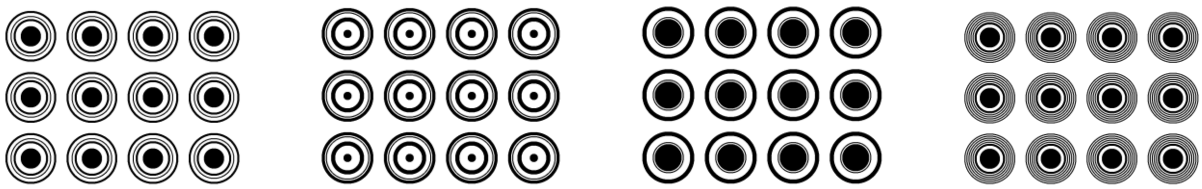

(a) division mask 1 *(b) division mask 2* *(c) division mask 3* *(d) division mask 4*

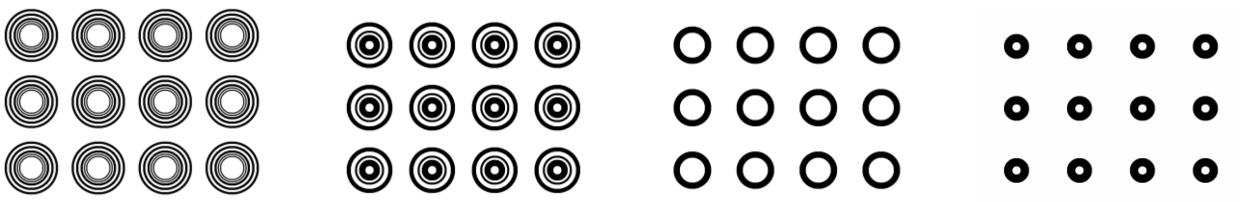

(e)division mask 5 *(f)division mask 6* *(g) division mask 7* *(h)division mask 8*

Fig. 13. Division masks for truncated cone.

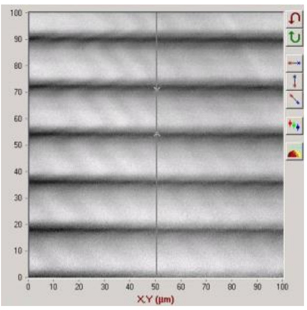

(a) Lithography pattern by using original grey mask

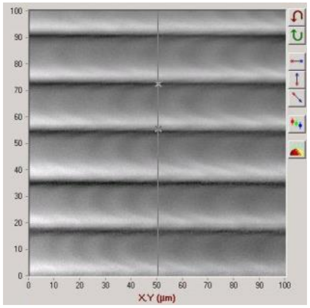

(b) Lithography pattern by using division masks

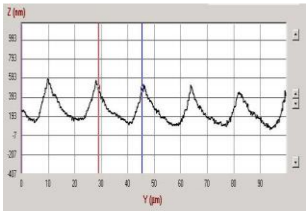

(c) 2D profile by grey exposure

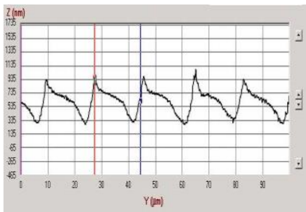

(d) 2D profile by division exposure

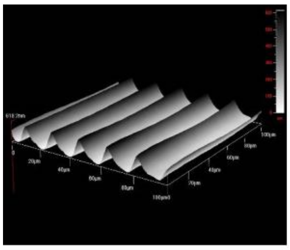

(e) 3D profile by grey exposure

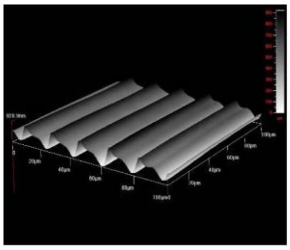

(f) 3D profile by division exposure

Fig. 14. Lithography patterns of zigzag grating.

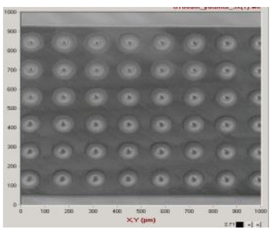

(a) Lithography pattern for truncated cone array

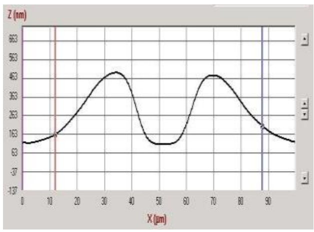

(b) 2D profile for truncated cone array

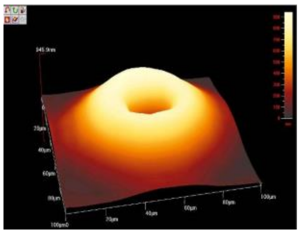

(c) 3D profile for truncated cone array

Fig. 15. Lithography patterns of truncated cone array.

4.3 Experiment combing periodic amplification with bit coding division

For some microstructure, which is similar to binary grating in horizontal direction (X) and is of gradual-change gray in vertical direction (Y), we obtain the better exposure patterns by using periodic amplification division in X direction and utilizing bit coding division in Y direction. Firstly, periodic amplification method is adopted. Then bit coding method is taken. Finally, twelve pieces of division masks are obtained as shown in Fig.16. Although masks in each column look the same, the difference among them is the position of lines in masks. In exposure process, the division masks are exposed row by row. The exposure time of Fig. 16(a1)~(d1) is 1s, 2s, 4s, 8s respectively, and are the same with the other two rows. The lithography results in Fig. 17 reveal that the method combining periodic amplification with bit coding division can be used to fabricate some special microstructure.

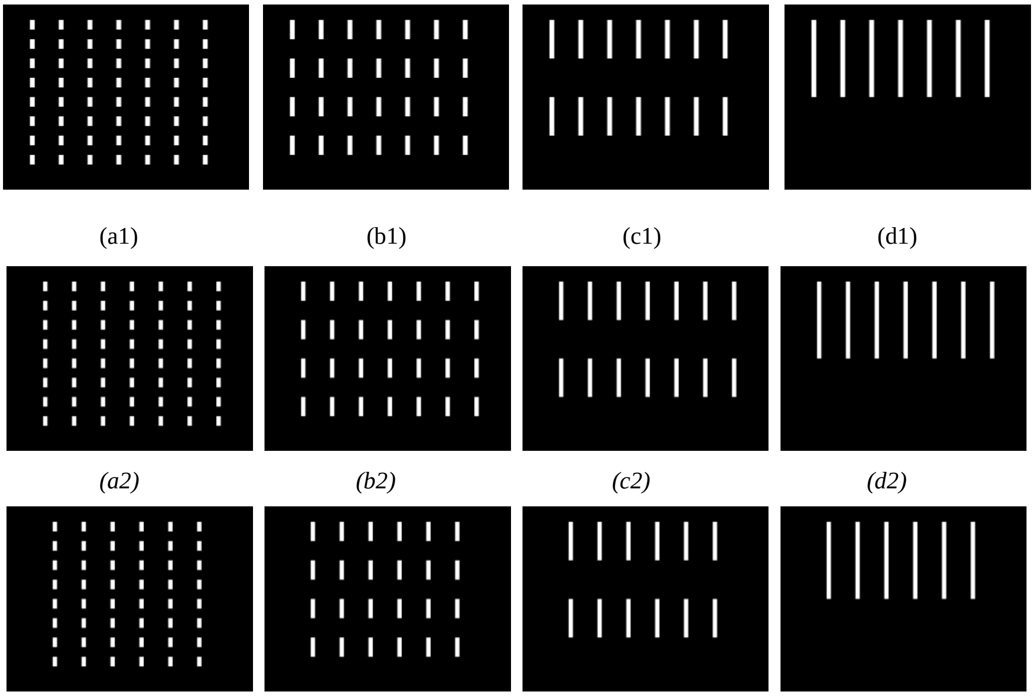

(a1) (b1) (c1) (d1)

(a2) (b2) (c2) (d2)

(a3) (b3) (c3) (d3)

Fig. 16. Division masks by combing periodic amplification with bit coding division.

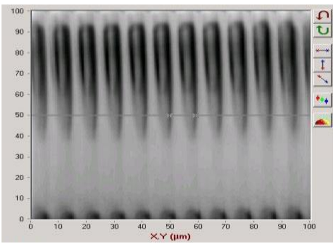

(a) Lithography pattern

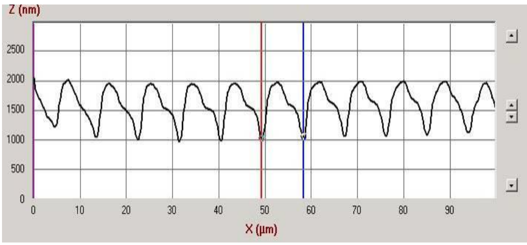

(b) 2D profile

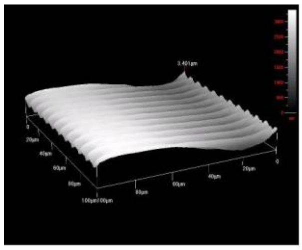

(c) 3D profile

Fig. 17. Lithography results.

5. Conclusions

Aiming at the low-pass property of reduction lens in DMD-based maskless lithography system, the digital division mask technique has been proposed to improve the lithography quality. Three division methods are developed, including periodic amplification division, bit coding division and the two combine. Some microstructures such as binary grating, zigzag grating, and truncated cone array have been fabricated by using the above methods. Theoretical analysis and experimental results prove that these proposed methods can enhance the high-frequency energy carrying edge information to some extent. Consequently, the edge sharpness of lithography pattern can be improved and the lithography quality can be promoted. However, the periodic amplification division is only effective for discrete periodic structure. For the bit coding division method by adopting superimposed exposure of multiple binary masks, the fabricated microstructure is just approximately continuous. So the bit coding division is not satisfied for the fabrication of complex microstructures with smooth continuous profile. Future work will be concentrated on the promotion of fabrication accuracy and the fabrication of complex microstructures by using these new methods.

Acknowledgments

The work was supported by the Chinese Nature Science Grant (60777046, and 61072131) and Innovation Fund for Aerospace Science (CASC201105).

References

[1] X. Zhang, X.N. Jiang, C. Sun, Sensors and Actuators **77**, 149 (1999).
[2] Terutake Hayashi, Takayuki Shibata, Takahiro Kawashima, Eiji Makino, Takashi Mineta, Toru Masuzawa, Sensors and Actuators A **144**, 381 (2008).
[3] M. V. Kessels, C. Nassour, P. Grosso, K. Heggarty, Optics Communications **283**, 3089 (2010).
[4] Kentaro Totsu, Kenta Fujishiro, Shuji Tanaka, Masayoshi Esashi, Sensors and Actuators A **130-131**, 387 (2006).
[5] Manseung Seo, Jaesung Song, Changgeun An, Lecture Notes in Computer Science **3926**, 108 (2006).
[6] Ningning Luo, Yiqing Gao, Min Chen, Lixia Yu, Qing Ye, Optica Applicata, **XL**(1), 239 (2010).

*Corresponding author: ningningluo2002@126.com